RADIATION AND INTERNAL CHARGING ENVIRONMENTS FOR THIN DIELECTRICS IN INTERPLANETARY SPACE

Joseph I. Minow
NASA/Marshall Space Flight Center, Huntsville, Alabama 35812 USA
Phone: +1-256.544.2850 Fax: +1-256.544.0242 Email: joseph.i.minow@nasa.gov

Linda Neergaard Parker, Richard L. Altstatt, William C. Blackwell, Jr., and Anne Diekmann
Jacobs Sverdrup, MSFC Group, Huntsville, Alabama 35812 USA

Abstract

Spacecraft designs using solar sails for propulsion or thin membranes to shade instruments from the sun to achieve cryogenic operating temperatures are being considered for a number of missions in the next decades. A common feature of these designs are thin dielectric materials that will be exposed to the solar wind, solar energetic particle events, and the distant magnetotail plasma environments encountered by spacecraft in orbit about the Earth-Sun L2 point. This paper will discuss the relevant radiation and internal charging environments developed to support spacecraft design for both total dose radiation effects as well as dose rate dependent phenomenon, such as internal charging in the solar wind and distant magnetotail environments. We will describe the development of radiation and internal charging environment models based on nearly a complete solar cycle of Ulysses solar wind plasma measurements over a complete range of heliocentric latitudes and the early years of the Geotail mission where distant magnetotail plasma environments were sampled beyond X_{GSE} = -100 Re to nearly L2 (X_{GSE} ~ -236 Re). Application of the environment models in example charging analyses demonstrate minimal but potential risks due to charging in interplanetary environments.

1.0 Introduction

Dielectric materials used in spacecraft construction can be the source of electrostatic discharges when charge is collected from the space environment at a rate faster than the excess charge deposited in the insulating material can be removed through conduction and electric fields associated with the buried charge density exceeds the dielectric breakdown strength of the material. Increasingly, dielectrics are finding their way into critical systems exposed to the space environments. Standard environment models for use in evaluating total radiation dose and dose rate effects in interplanetary space rarely extend to low energies below a few MeV because they are intended for use in computing effects of very energetic ions accelerated during solar particle events to energies of 10's to 100's MeV. Ions with these energies penetrate significant thicknesses of shielding and are capable of depositing charge deep in materials and producing upsets in electronic parts, but the particle flux at these high energies are typically insufficient to produce dose rate effects including internal charging or contribute significant total dose to materials near the surface and so are generally not considered to be an issue for material degradation.

Spacecraft systems design for a number of missions in the next few decades are using solar sails for propulsion [*Drexler,* 1979; *Forward*, 1999; *West and Derbes*, 2000; *Garbe and Montgomery*, 2003], thin membranes to shade instruments from the sun to achieve cryogenic operating temperatures for infrared instrumentation [*Woolf and Angel*, 2000; *Johnston et al.*, 2001], and other light weight structural and propulsion design elements to reduce total vehicle mass [*Forward*, 1999]. A design feature common to a number of these systems are 10^2 to 10^4 m^2 areas of dielectric material with thickness ranging from less than 1μm to a few 10's μm and the potential for applications of dielectric materials at cryogenic temperatures with feature sizes ranging from 0.1 to 1 cm or larger. These materials will be exposed to solar wind and solar energetic particle event environments over a range distances from the Sun from less than 0.5 AU to beyond Earth orbit at the Earth-Sun L2 point (X_{GSE} = -236 Re or 1.01 AU from the Sun). In addition, spacecraft in orbit about the Earth-Sun L2 point will be exposed to plasma environments of the Earth's distant magnetosheath and magnetotail. While outside of the harsh internal charging environments of the Earth's radiation belts, these missions must still evaluate the potential effects of interplanetary radiation environments on the dielectric materials. Electron flux at energies of from 10's to 100's keV, which are stopped by thin dielectrics can

be significant in interplanetary environments, may approach the levels sufficient to produce internal charging effects and significant radiation damage over the length of a mission.

This paper describes the development and preliminary applications of solar wind and distant magnetotail plasma models for use in evaluating the radiation damage to materials and potential internal charging threats to dielectric structures exposed to interplanetary space environments. A technique for creating statistical charged particle environment models from plasma moments and differential flux is described using archived data from research spacecraft. The modeled environments are then used to provide directional electron flux onto exposed dielectric surfaces for sample internal charging applications to demonstrate the conditions for which interplanetary space environments are benign and where potential charging risks may exist.

2.0 Model Construction

Charged particle flux environments for interplanetary space are constructed using standard techniques for modeling differential flux spectra from plasma moments [c.f, *Chan et al.*, 1977; *Garrett and DeForest*, 1979; *Kane et al.*, 1995] and constraining the high-energy, non-thermal tails with energetic flux measurements [*Garrett and Hoffman*, 2000; *Collier et al.*, 1996; *Maksimovic et al.*, 1997; *Chotoo et al.*, 1998]. Plasma number density N_i, temperature T_i, and bulk velocity $V_{C,i}$ moments for each species (i=electron, proton, or helium) are used to compute Maxwellian distribution functions for the i^{th} species $f_{M,i}$

$$f_{M,i}(\mathrm{v}) = \frac{n_i}{\left(\sqrt{\pi}\theta_{M,i}\right)^3} \exp\left[-\left|\mathrm{v} - \mathrm{V_c}\right|^2 \Big/ \theta^2_{\mathrm{M,i}} \right] \qquad \theta_{M,i} = \sqrt{\frac{k_B T_i}{m_i}} \tag{1}$$

and Kappa distribution functions $f_{\kappa,i}$

$$f_{\kappa,i}(\mathrm{v}) = \frac{n_i}{\left(\sqrt{\pi}\theta_{\kappa,i}\right)^3} \frac{\Gamma(\kappa_i + 1)}{\sqrt{\kappa_i^3}\,\Gamma(\kappa_i - \frac{1}{2})} \left[1 + \frac{\left|\mathrm{v} - \mathrm{V}_c\right|^2}{\kappa_i \theta^2_{\kappa,i}} \right]^{-(\kappa+1)} \qquad \theta_{\kappa,i} = \sqrt{\frac{(2\kappa - 3)k_B T_i}{\kappa_i m_i}} \tag{2}$$

where k_B is Boltzman's constant, $\Gamma(x)$ is the gamma function, m_i the mass of species i, θ is the core thermal speed of the distributions [*Collier et al.*, 1996], and κ_i is the Kappa parameter which must satisfy $\kappa_i > 3/2$ for all species. It is frequently advantageous to use bi-Maxwellian or even combinations of Maxwellian and Kappa distributions to reconstruct the differential flux from plasma moments. Differential flux dJ/dE for species i (units of #/cm^2-sec-sr-Joule) is derived from the distribution function f_i (units of #s^3/m^6) using the relationship

$$\frac{dJ_i}{dE} = \frac{\mathrm{v}^2}{\mathrm{m_i}} f_i(\mathrm{v}) \tag{3}$$

The technique assumes the appropriate Maxwellian or Kappa moments are available and at least the number density, bulk velocity, and temperature moments are derived from least square fits to the distribution functions [c.f., *Garrett and DeForest*, 1979; *Garrett et al.*, 1981]. In many cases investigators provide bi-Maxwellian or even more sophisticated multi-dimensional moments derived from least square fits of distribution functions to the data and reasonable representations of the original differential flux environments can be reconstructed from the moment data even if the original distribution functions are truncated. When the moment integrals are approximated by discrete sums over the measured distribution functions instead of using least square fitting algorithms the resulting moments are more susceptible to noise in the differential flux measurements and are biased due to truncation of the distribution functions by the finite energy range of the detector system [*H.B. Garrett*, personal communication, 2005]. Internal charging environments in particular require good representation of the particle flux in the non-thermal tails of the energy spectra at energies greater than 100 keV and the environments are often poorly reconstructed at these energies if the maximum energy of the detector system is only a few 10's keV even if fits were conducted over the limited range of energies near the peak of the distribution function. For the applications reported here, the non-thermal tails of the Kappa distributions which provide the internal charging environments are constrained by using differential flux measurements at energies from 100 keV to 1000 keV assuring the environments are appropriate for internal charging analyses.

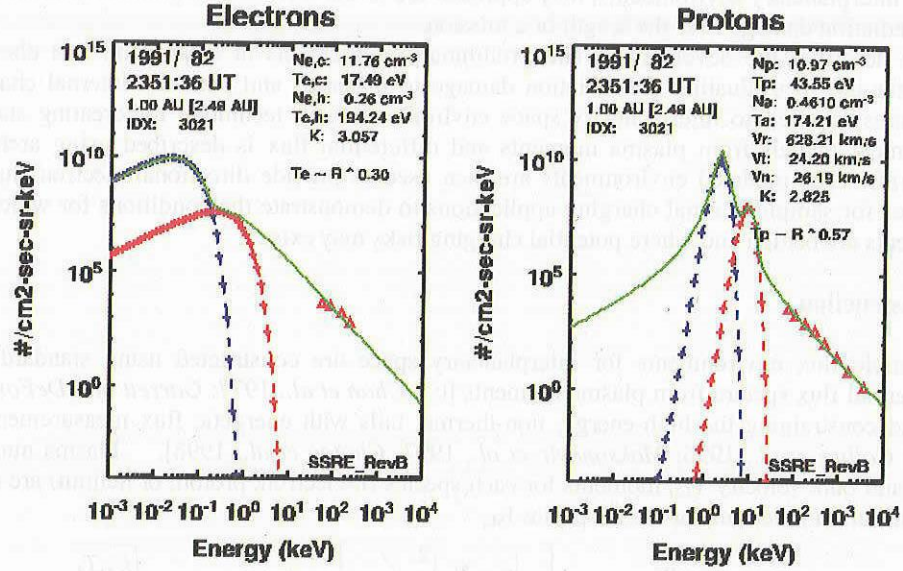

(a) (b)

Figure 1. Reconstructed Ulysses Solar Wind Differential Flux Spectra. (a) Electron spectra are composed of Maxwellian core (blue dashed line) and halo (dashed red line) populations with an energetic electron flux (red triangles) that constrain the non-thermal tail of the distribution. The modeled electron environment (green line) is the sum of the Maxwellian core with a Kappa representation of the halo constrained by the energetic electron distribution. (b) Ion populations are modeled (green) as a sum of Kappa proton and helium ion distributions. Individual Maxwellian proton (dashed blue) and helium (dashed red) spectra are shown with the energetic proton flux measurements (red triangles).

2.1 Ulysses Solar Wind Model

Plasma moments and energetic particle instruments from the Ulysses spacecraft are used to characterize solar wind environments for a wide range of heliospheric latitudes. The spacecraft is in a 1.3 AU by 5.2 AU orbit about the Sun that is inclined 80° from the ecliptic plane. Ulysses is the only spacecraft to date that has sampled high latitude solar wind environments far from the ecliptic plane. Ulysses plasma and energetic particle records are therefore uniquely capable of providing information necessary for defining radiation and charging environments for the Solar Polar Imager mission currently in development that is planned to utilize solar sail propulsion technology at high solar latitudes at a distance of 0.5 AU from the Sun. The Solar Wind Observations Over the Poles of the Sun (SWOOPS) instrument [*Bame et al.*, 1992] provides the low energy electron and ion component of the solar wind and the Low-Energy Magnetic Spectrometer (LEMS) and Low Energy Foil Spectrometer (LEFS) instruments from the Ulysses Heliosphere Instrument for Spectra, Composition, and Anisotropy and Low Energies (HISCALE) experiment [*Hunt-Ward and Armstrong*, 2003] provide ion and electron environments at energies from a few 10's keV to a few MeV are used to derive the environment. Data used in the radiation model are one hour averages of appropriate plasma moments and energetic particle flux interpolated to a uniform time base.

Figure 1 provides an example application of the technique to construct differential electron and ion flux spectra over an energy range from 10^{-3} keV to 10^{4} keV using Ulysses' SWOOPS, LEMS, and LEFS measurements from day 82 of 1991. Electron differential flux spectra are constructed by summing a Maxwellian velocity distribution function representing the core (blue line) and a Kappa velocity distribution function (green line) for the halo and "super-halo" components of the electron population. SWOOPS core electron density $N_{e-,c}$ and temperature $T_{e-,c}$ and halo electron density $N_{e-,h}$ and temperature $T_{e-,h}$ parameters along with the radial component of the solar wind convection velocity V_r are used in both distribution functions. κ parameters are varied until the differential electron flux halo population matches the LEMS and LEFS differential electron flux measurements within a predefined tolerance. Energetic particle flux at energies of importance to internal charging is therefore constrained by the LEMS and LEFS differential electron flux measurements.

Ion differential flux spectra in Figure 1-b are similarly constructed from the Kappa distribution function using SWOOPS plasma moments for the proton density N_{H+} and temperature T_{H+} and helium density N_{He++}. A single, common solar wind convection velocity is reported for all ion and electron species in the SWOOPS moments. In the current version of the model, only the dominant radial component V_r of the convection velocity $\mathbf{V_c} = V_r\,\mathbf{r} + V_t\mathbf{t} + V_n\mathbf{n}$ (in the heliocentric radial, tangential, normal coordinate system) is used because the tangential and normal components are typically small compared to the radial component of the solar wind flow. The κ parameter that defines the high energy tail of the Kappa distribution function is not available in the SWOOPS plasma moments but is obtained by adjusting the κ parameter to constrain the computed differential proton flux to match the measured LEMS30 and LEM120 energetic proton flux values at high energies.

SWOOPS plasma moments do not include helium temperature so an assumption that $T_{He++} \approx T_{H+}$ is used to derive the helium differential flux. The κ parameter derived from proton moments and energetic proton flux is similarly adopted for the helium environment as well. Figure 1b provides an example of a proton Maxwellian energy spectra computed from Ulysses proton moments (red line) that is merged with energetic proton flux at high energies by constraining the tail of the Kappa function (green line) to match the measured energetic proton flux values.

The radius of the Ulysses spacecraft orbit varied from 1.0 AU to 5.4 AU from the Sun during the outbound voyage from the Earth to Jupiter and approximately 1.3 AU to 5.4 after Jupiter fly-by in 1992. Solar wind environments are therefore always sampled by Ulysses at radial distances from the Sun greater than 1 AU and the bulk of the information is from greater than 1.3 AU. Cold plasma moments and particle flux have been scaled from the spacecraft location to 0.5 AU or 1.0 AU based on scaling laws that have been derived from scientific studies of solar wind summarized in *Burlaga* [1995]. Solar wind velocity is independent of radial distance and the radial dependence of solar wind density and temperatures adopted to scale Ulysses solar wind parameters are R^{-2} for electron and ion density, $R^{-0.57}$ for ion temperatures, and $R^{-0.30}$ for electron temperatures [*Burlaga*, 1995].

Scaling LEMS and LEFS energetic ion, electron differential flux measurements is problematic. Treatments based on interplanetary magnetic field "flux tube" volumes have been suggested where radial extrapolations should be implemented using the following R^N radial variations [*Feynman and Gabriel*, 1988]

- Flux extrapolations from 1 AU to >1 AU should use $N = -3.3$ and expect $-4 \le N \le -3$ variations,
- Flux extrapolations from 1 AU to <1 AU should use $N = -3.0$ and expect $-3 \le N \le -2$ variations,
- Fluence extrapolations from 1 AU to other distances should use $N = -2.5$ and expect $-3 \le N \le -2$ variations.

More recently, *Smart and Shea* [2003] argue that simple power laws of any type may be misleading for coronal mass ejection sources that provide the extreme flux events in interplanetary space. The mean values of $N = -3.3$ and $N = -3.0$ for >1 AU and <1 AU, respectively, are adopted for Solar Sail Radiation Environment (SSRE) Revision B (SSRE-RevB), the current version of the solar wind flux model.

Using the process just described, an individual differential flux spectrum is computed over an energy range from 0.01 keV to 10 MeV in 73 energy steps for each set of the one hour averaged electron and ion records in the Ulysses data set yielding a set of 110,572 hourly records over a 12.6 year period. Figure 2 provides an example of SSRE-RevB for positive flux (in the direction of the solar wind) for the complete Ulysses data set in a spectrogram format with time on horizontal axis, energy on the vertical axis, and the differential flux indicated by the color bars.

Figure 2 provides a reconstructed Ulysses solar wind differential flux in the direction of the radial component of the solar wind flow summarizing the environments used in the SSRE-RevB model. The format of the plot is Universal time (in decimal years) on the horizontal axis, particle kinetic energy on the vertical axis, and differential flux intensity indicated by the color scale. Any flux value greater than the 1.0×10^{12} #/cm^2-s-sr-keV maximum flux threshold or less than the 1.0×10^{2} #/cm^2-s-sr-keV minimum threshold is set to white.

Both protons and helium are included in the ion environment shown in the top panel of Figure 2. Protons are the dominant ion in the solar wind flow representing approximately 95% to 97% of the number density while helium is typically only 3% to 5% of the solar wind. Other heavy ions are present as well in the solar wind (including carbon, nitrogen, oxygen, neon, magnesium, silicon, and iron) but typically ions heavier than helium only account for approximately ≤1% of the total composition of solar wind ions [*Ogilvie and Coplan*, 1995] and have therefore been neglected in the SSRE-RevB model environment.

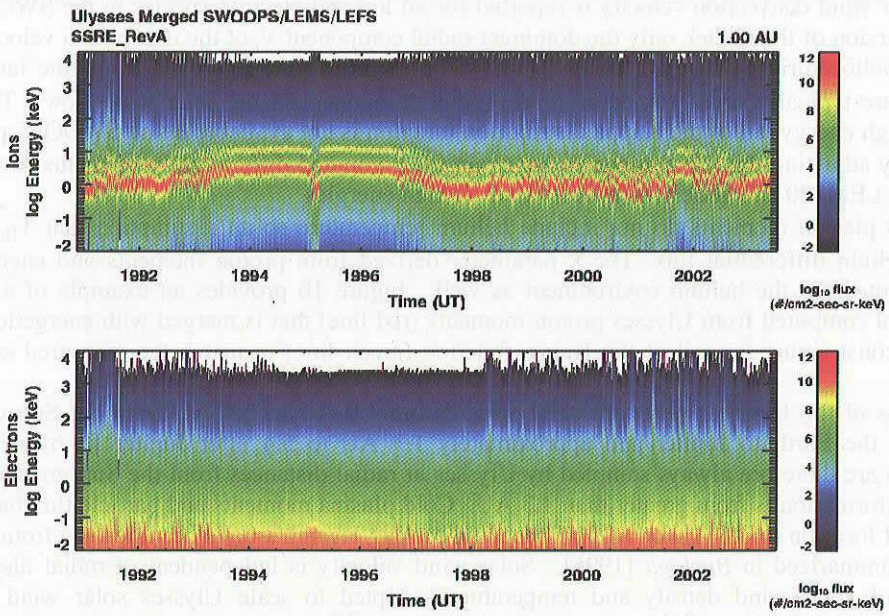

Figure 2. SSRE-RevA Positive Flux Reconstructed Environment. Ions (top panel) and electrons (bottom) panel are reconstructed from Ulysses solar wind plasma and energetic particle environments. The ion environment includes both hydrogen and helium ions.

The SSRE models provide only the free field charged particle environment. Due to spacecraft charging and plasma wake effects the differential flux near the sail are modified and these effects are not included in the environment model. Significant fluxes of photoelectrons emitted from the sail should only extend to energies of a few 10's eV and perturbations of the solar wind plasma by anticipated spacecraft potentials of positive tens of volts should only impact solar wind particles at energies on the order of a few 10's eV or less. Therefore, use of the environment for radiation testing and evaluation of internal charging due to particles with energies exceeding 1 keV is acceptable.

Statistical flux spectra are derived from the reconstructed spectra by sorting differential flux within individual energy bins into monotonically increasing flux values and extracting the flux value which occurs n% of the way through the file where n%=50%, 90%, 95%, 99%, and 100%. The final 100% value represents the maximum flux occurring in the record. Computing the percentile flux values for each energy bin yields a statistical flux as a function of energy for each of the percentile values. Figure 3 shows the electron and ion statistical differential flux in both the direction of the solar wind (solid lines) and the direction opposite the solar wind (dotted line). There is little difference in the electron environment for the two directions since the electron thermal energy dominates the energy associated with the convective motion of the plasma. Differences between the two environments are only apparent at the energies less than 1 keV. The "shoulder" in the electron spectra from 0.1 keV to 0.5 keV is due to contributions from the Maxwellian core electron population during periods of high solar wind velocity and the second "shoulder" from 1-10 keV is due to the peak in the Kappa distribution representing the halo electron population.

Ion environments are fundamentally anisotropic since the mean radial component of the solar wind convective motion (approximately 468 km/sec) dominates ion thermal velocities (typically only 30-60 km/sec). Multiple peaks occur in the statistical ion environment due to the effects of high and low speed solar wind environments and contributions from the multiple ion species. The peak with the highest flux in the 50% and 90% environments is due to low speed solar wind protons and the secondary peak is likely a combination of both high speed protons and low speed helium ions. The third peak at energies of 10 keV to 20 keV is due to helium ions in the high speed solar wind.

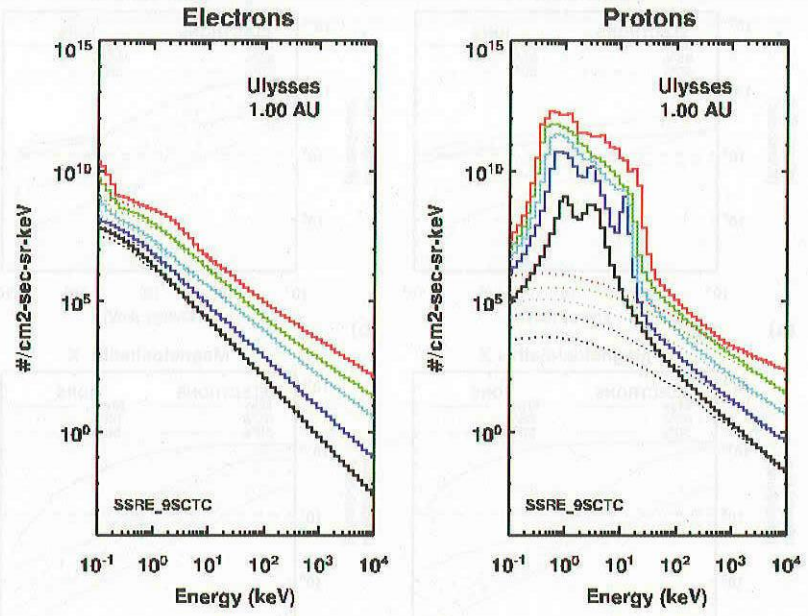

Figure 3. SSRE-RevA Differential Statsitical Flux. (a) Electron and (b) ion differential flux from energies of 0.1 keV to 1 MeV. Color coding indicates the 50% (black), 90% (blue), 95% (green), 99% (orange), and maximum (red) flux environments. Differential flux to a surface in the direction (opposite) of the solar wind flow is indicated by the solid (dotted) lines.

2.2 L2-Charged Particle Environment Model

Using similar techniques described above for the solar wind environment model, *Blackwell et al.* [2000] and *Minow et al.* [2000] developed an empirical engineering model of the L2 Radiation (LRAD) environment for species with energies <1 MeV. The original LRAD model is based on a restricted set of six months of Geotail spacecraft data, and it used Maxwellian distribution functions derived from Comprehensive Plasma Instrument Hot Plasma Analyzer (CPI/HPA) moments to obtain the particle flux statistics at energies less than a few 10's keV in each of the distant magnetotail plasma regimes and the statistical fluence spectra accumulated over complete halo orbits about L2. The LRAD model was intended primarily for use in estimating radiation total dose effects for materials on spacecraft orbiting about L2.

The L2-Charged Particle Model (L2-CPE) is a revised version of LRAD [*Minow et al.*, 2004] incorporating a number of new features. An updated, complete set of CPI/HPA plasma moments (including data from October 1992 through the end of 1994) was provided by the CPI/HPA principal investigator at the University of Iowa. The more extensive set of measurements replaces the six month, partial set used for the LRAD plasma moment database. Non-thermal ion and electron flux is included in L2-CPE using the corresponding energetic particle flux measurements from Geotail's Energetic Particle and Ion Composition Ion Composition Subsystem (EPIC/ICS) instrument to constrain the high energy tails of the Kappa distribution functions in the same way the LEMS and LEFS data was used in the Ulysses model. Solar wind environments in L2-CPE include two IMP-8 derived models from 1992 and 1995 solar maximum and minimum conditions, respectively, as well as solar maximum and solar minimum Ulysses solar wind environments.

Distant magnetotail environments included in L2-CPE are derived from Geotail CPI/HPA and EPIC/ICS measurements during the period October 1992 through October 1994 when the orbit of the Geotail spacecraft orbit allowed sampling of magnetoail and magnetosheath plasma regimes at distances from -50 Re $\leq X_{GSE} \leq$ -230 Re. Identification of the plasma regime (solar wind, magnetosheath, plasma mantle, boundary layer, lobe, plasma sheet) associated with each set of plasma moments and flux measurements was provided by the EPIC Science Team (*Christon et al.*, 1998; *Eastman et al.* 1998). All data within individual plasma regimes are combined independent of radial distance from the Earth to estimate variations in the L2 plasma parameters. This assumption is appropriate

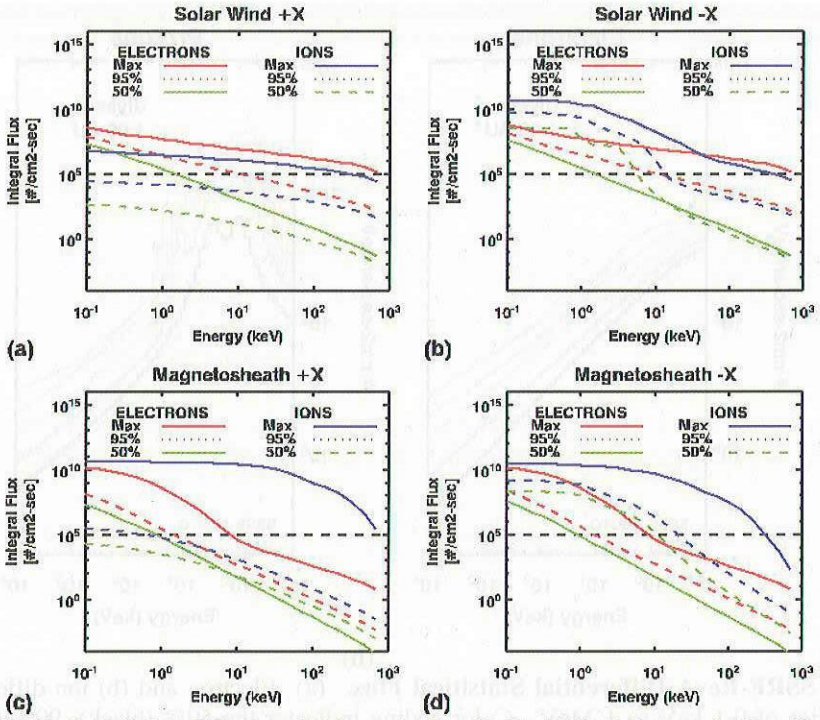

Figure 4. Statistical Solar Wind and Magnetosheath Statistical Integral Flux Environments. L2-CPE model flux environments are given for the 50%, 95%, and the maximum (100%) percentile levels for the solar wind IMP-8 solar maximum (1992) environment (a) opposite and (b) in the direction of the solar wind flow. Corresponding statistical environments for the magnetosheath are shown in (c) and (d). Flux of 1.0×10^5 #/cm^5-sec is marked by the horizontal black dashed line.

for an engineering model since no obvious radial variations in plasma density, temperature, and velocity parameters were identified in the database.

Relatively few solar wind encounters are included in the Geotail data set at distances beyond $X_{GSE} \leq -50$ Re. Plasma moments from the Interplanetary Monitoring Platform (IMP) 8 Faraday Cup experiment from 1992 and 1995 solar maximum and minimum conditions, respectively, are used instead for the solar wind environments. The IMP-8 spacecraft is in a near circular 35 Re orbit about the Earth, but the solar wind parameters are still appropriate for L2 since variations in plasma parameters as a function of radial distance from Earth to L2 are sufficiently small (on the order of a few percent or less) that near Earth solar wind values were simply adopted for L2 without any attempts to correct for radial distance. This assumption yields a model with conservative flux estimates on the order of a few percent greater than actual solar wind values.

Integral directional flux spectra from L2-CPE are shown in Figure 4 for the solar wind and magnetosheath environments and Figure 5 for the plasma mantle (including the plasma boundary layers and lobe regimes) and plasma sheet. Anisotropies are present in the solar wind and magnetosheath ion environments due to the large bulk flow velocities compared to the much smaller ion thermal velocity while electrons are isotropic for all of the environments.

3.0 Application to Internal Charging

Dielectric response to exposure to electron environments in the solar wind and the distant magnetotail can now be evaluated using the integral flux environments from the SSRE and L2-CPE models. Analysis of Combined Radiation and Release (CRRES) Internal Discharge Monitor (IDM) Experiment [*Frederickson et al.*, 1993] has shown that insulating materials generally do not exhibit discharge pulses when exposed to geostationary transfer orbit electron environments unless the energetic electron flux exceeded values of 1×10^5 to 5×10^5 electrons/cm^2-sec [*Frederickson et al.*, 1991, 1992]. The IDM Experiment was shielded by 0.2 cm aluminum which stopped all electrons <150 keV and passed unimpeded electrons >1 MeV. Additional data obtained during later periods in the

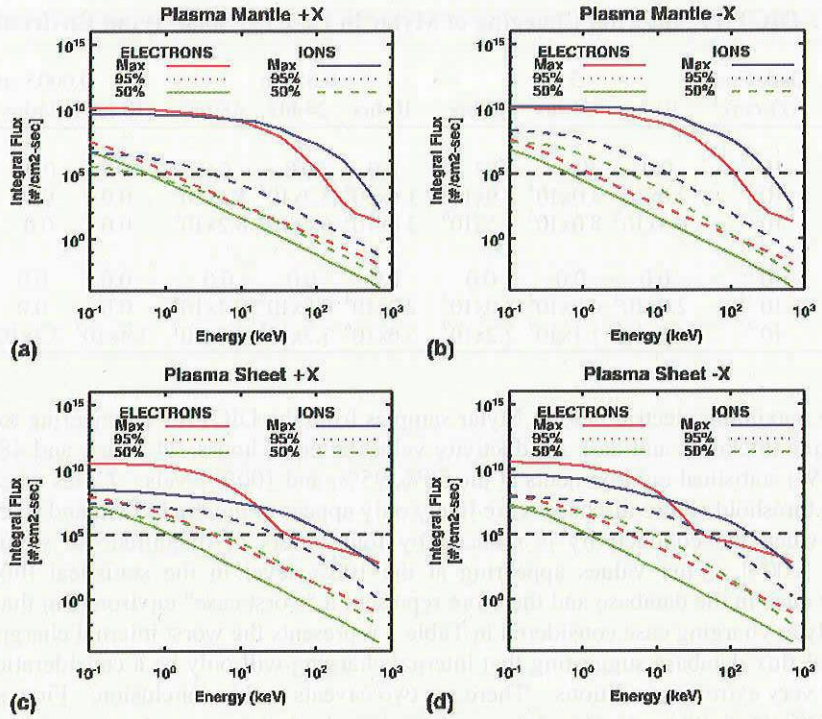

Figure 5. Statistical Plasma Mantle and Plasmasheet Statistical Integral Flux Environments. L2-CPE model flux environments are given for the 50%, 95%, and the maximum (100%) percentile levels for the plasma mantle environment (a) opposite and (b) in the direction of the solar wind flow and corresponding statistical plasma sheet environments for the magnetosheath are shown in (c) and (d). Flux of 1.0×10^5 #/cm^5-sec is marked by the horizontal black dashed line.

CRRES mission suggested it was more prudent to reduce the "safe flux" level to 1×10^5 electrons/cm^2-sec when additional pulses were observed at lower electron fluences per orbit [*Frederickson et al.*, 1992]. The flux threshold for MeV electrons incorporated into the NASA internal charging guidelines [*HDBK-4002*, 1999] is based on these results. However, it should be noted that the 1×10^5 electrons/cm^2-sec threshold assumes the insulating materials are shielded reducing the flux of 150 keV to 1 MeV electrons which can deposit significant charge in thin materials and the insulating materials are at ambient temperatures with "high" electrical conductivities that may be significantly reduced at low temperatures.

Swaminathan et al. [2004] compared conductivity measurements of 51 μm thick Kapton H material [*Sheldahl*, 2003] with 0.1 μm vapor deposited aluminum at ~299°K using traditional methods in ambient room light and humidity, they compared the results with the charge storage method [*Frederickson*, 2003] that provides a more relevant space environment test. The classical result yielded ~3.3×10^{-17} $(\Omega\text{-cm})^{-1}$ consistent with the published value of 1×10^{-17} $(\Omega\text{-cm})^{-1}$ provided by the manufacturer compared to the charge storage method result at room temperature of $<2 \times 10^{-20}$ $(\Omega\text{-cm})^{-1}$. Reduced material temperatures in cryogenic applications could produce further reductions in the dark conductivity of many polymers to even lower values.

We now present an example application of the L2 environment model in estimating the electric fields generated by internal charging in Mylar, a common material used in lightweight spacecraft design. Electric field results using standard conductivity values are compared to electric fields obtained with the standard value reduced by four orders of magnitude to simulate either the reduced conductivities reported in the charge storage measurements or low temperature reductions in dark conductivity. Integral >100 keV electron flux in the L2 environments presented in Figures 4 and 5 exceed the 1×10^5 electrons/cm^2-sec threshold flux only in the maximum (100%) solar wind and plasma mantle environments. The L2-CPE solar wind environment is a good case because it represents both an extreme environment for spacecraft orbiting L2 and can be used to represent environments for spacecraft at L1. Accordingly, the 50%, 95%, and 100% (worst case) flux values from the solar wind environment are considered here. The material geometry is a planar unshielded dielectric mounted on a grounded metal surface with a direction flux of electrons incident on the dielectric surface.

Table 1. DICTAT Internal Charging of Mylar in L2-CPE Solar Wind Environment

Environment	Dark Cond.	5 cm			0.05 cm			0.0005 cm		
	$(\Omega\text{-cm})^{-1}$	10-hrs	24-hrs	48-hrs	10-hrs	24-hrs	48-hrs	10-hrs	24-hrs	48-hrs
50% SW	10^{-18}	0.0	0.0	0.0	0.0	0.0	0.0	0.0	0.0	0.0
95% SW	10^{-18}	2.0×10^{4}	4.0×10^{4}	5.9×10^{4}	1.6×10^{4}	3.2×10^{4}	5.4×10^{4}	0.0	0.0	0.0
100% SW	10^{-18}	8.3×10^{6}	8.0×10^{6}	9.5×10^{6}	3.4×10^{6}	6.4×10^{6}	8.2×10^{6}	0.0	0.0	0.0
50% SW	10^{-22}	0.0	0.0	0.0	0.0	0.0	0.0	0.0	0.0	0.0
95% SW	10^{-22}	2.0×10^{4}	4.0×10^{4}	8.0×10^{4}	2.0×10^{4}	4.8×10^{4}	9.4×10^{4}	0.0	0.0	0.0
100% SW	10^{-22}	4.8×10^{6}	1.1×10^{7}	2.2×10^{7}	5.6×10^{6}	1.3×10^{7}	2.6×10^{7}	1.4×10^{5}	3.3×10^{5}	6.6×10^{5}

Table 1 gives the maximum electric field in Mylar samples from the DICTAT engineering tool [Rodgers, 1999] as a function of sample thickness and dark conductivity values after 10 hours, 24 hours, and 48 hours exposure to the L2 solar wind (SW) statistical environments at the 50%, 95%, and 100% levels. Cases where the electric field exceeds the 10^7 V/m threshold where discharges are likely only appear in the thick 5 cm and 0.05 cm samples at the 100% environment when the conductivity is reduced by four orders of magnitude to simulate the results of *Swaminathan et al.* [2004]. Flux values appearing at the 100% level in the statistical flux environments by definition occur only once in the database and therefore represent a "worst case" environment that persists for only a few records. The Mylar charging case considered in Table 1 represents the worst internal charging environments in the L2-CPE statistical flux database suggesting that internal charging will only be a consideration for spacecraft in orbit about L2 under very extreme conditions. There are two caveats to this conclusion. First, simply reducing the conductivity to 1×10^{-22} $(\Omega\text{-cm})^{-1}$ to simulate low conductivities in the space environment may underestimate the magnitude of the problem. Materials may exhibit even lower conductivities if the charge storage values are combined with temperature reductions. Further reductions in conductivity was not considered because the current version of DICTAT has a lower limit of 1×10^{-22} $(\Omega\text{-cm})^{-1}$ for dark conductivity values. Second, there are additional events in the Geotail/IMP-8 data set (the basis of the L2-CPE model) that are not included in the current version of the L2-CPE code. These events are being evaluated to determine if they represent credible worst case charging environments or are simply spurious values due to energetic ion contamination of electron sensors and the results will be reported elsewhere. Further analysis of the charging environments are required to determine if there are internal charging threats for spacecraft in solar wind or L2 environments.

4.0 Summary

Environment models for use in characterizing the interplanetary charged particle environments over an energy range from 0.1 keV to >1 MeV have been developed. The Solar Sail Radiation Environment (SSRE) model was derived from Ulysses plasma and energetic particle flux measurements scalable to a wide range of radial distances from the Sun. Primarily intended for use in estimating surface radiation dose and dose as a function of depth in thin materials, the model also provides statistical flux environments that can be used to assess internal charging threats. Similarly, the L2-Charged Particle Environment (L2-CPE) model was developed to provide radiation dose estimates for spacecraft in orbit about L2 but can also be used to provide statistical estimates of flux within the solar wind, magnetosheath, plasma mantle, and plasma sheet over a range of distances from -50 Re < XGSE < L2 at -236 Re.

An example DICTACT charging analysis of Mylar exposed to solar wind charging environments from the L2-CPE model, the most extreme internal charging environment provided by the current version of L2-CPE, suggests that threats to internal charging are only a potential concern in the most extreme case of reduced conductivity at the 100% environment. However, further work is required to fully characterize the properties of the models. Because they were developed to give mean environments with statistical information on the deviations about the mean, the best use of the current versions are for estimates of mission dose and mean charging conditions where the 50% environments drive the physics of the radiation interactions. Updates to the models are anticipated in the future when the properties of the extreme environments are more fully understood and can be incorporated into the models.

Acknowledgements

We thank Dr. L. Lanzerotti (HISCALE) and Dr. D.J. McComas (SWOOPS) for making Ulysses data available through the National Space Science Data Center and acknowledge the contributions of Dr. B. Goldstein for

providing the SWOOPS plasma moments. Dr. R. McEntire provided the Geotail EPIC/ICS data and Dr. W. Peterson the CPI/HPA data. IMP-8 data is obtained courtesy of Dr. A. Lazarus. This work was supported in part by the In Space Propulsion Program at MSFC and NASA's Space Environments and Effects Program.

References

Bame, S.J., D.J. McComas, B.L. Barraclough, J.L. Phillips, K.J. Sofaly, J.C. Chavez, B.E. Goldstein, R.K. Sakurai, The Ulysses Solar Wind Plasma Experiment, Astronomy and Astrophysics, Supplement Series, Ulysses Instruments Special Issue, Vol. 92, 237 – 265, 1992.

Blackwell, W.C., J.I. Minow, S. W. Evans, D.M. Hardage, and R.M Suggs, "Charged particle environment definition for NGST: Model development," in *UV, Optical, and IR Space Telescopes and Instruments, Proc. SPIE*, **4013**, J.B. Breckinridge and P. Jakobsen, eds., pp. 908 – 919, 2000.

Burlaga, L.F., Interplanetary Magnetohydrodynamics, Oxford University Press, 1995.

Chan, K. W., K.W. Sawyer, J.I. Vette, A model of the near-earth plasma environment and application to the ISEE-A and -B orbit, NASA-TM-X-72611 (NSSDC/WDC-A-R/S-77-01, 19770701), July, 1977.

Christon, S.P., T.E. Eastman, T. Doke, L.A. Frank, G. Gloeckler, H. Kojima, S. Kokubun, A.T.Y. Lui, H. Matsumoto, R.W. McEntire, T. Mukai, S.R. Nylund, W.R. Paterson, E.C. Roelof, Y. Saito, T. Sotirelis, K. Tsuruda, D.J. Williams, and T. Yamamoto, Magnetospheric plasma regimes identified using Geotail meausrements 2. Statistics, spatial distribution, and geomagnetic dependence, *J. Geophys. Res., 103, 23521 – 23542, 1998.*

Chotoo, K., M.R. Collier, A.B. Galvin, D.C. Hamilton, and G. Gloeckler, Extended solar wind helium distribution functions in high-speed streams, JGR, 103, 17,441 – 17,445, 1998.

Collier, M.R., D.C. Hamilton, G. Gloeckler, P. Bochsler, and R.B. Sheldon, Neon-20, oxygen-16, and helium-4 densities, temperatures, and suprathermal tails in the solar wind determined with WIND/MASS, Geophys. Res. Lett., 23, 1191-1194, 1996.

Drexler, K.E. High performance solar sails and related reflecting devices, AIAA Paper 79-1418, 4th AIAA Conference on Space Manufacturing Facilities, Princeton University, Princeton, N.J., May 14-17, (1979).

Eastman, T.E., Christon, S.P., T. Doke, L.A. Frank, G. Gloeckler, H. Kojima, S. Kokubun, A.T.Y. Lui, H. Matsumoto, R.W. McEntire, T. Mukai, S.R. Nylund, W.R. Paterson, E.C. Roelof, Y. Saito, T. Sotirelis, K. Tsuruda, D.J. Williams, and T. Yamamoto, Magnetospheric plasma regimes identified using Geotail meausrements 2. Regime identification and distant tail variability, *J. Geophys. Res.*, 103, 23521 – 23542, 1998.

Evans, S.W. (editor), "Natural Environments Near the Sun-Earth/Moon L2 Libration Point," NASA, MSFC, 2000.

Forward, Robert, Gossamer Spacecraft Survey Study, Preliminary Report - Historical Survey, Forward Unlimited, Clinton, WA, 1999.

Feynman, J., and S. Gabriel (Eds.), Interplanetary Particle Environment, JPL Publication 88-28, Jet Propulsion Laboratory, California Institute of Technology, Pasadena, CA, 1988.

Frederickson, A.R., Measurement of conductivity and charge storage in insulators related to spacecraft charging, IEEE Trans. Nuc. Sci., 50, 2003.

Frederickson, A.R., E.G. Holeman, and E.G. Mullen, Characteristics of Spontaneous Electrical Discharging of Various Insulators in Space Radiations, IEEE Trans. Nuc. Sci., 39, 1773 – 1782, 1992.

Frederickson, A.R., E.G. Mullen, D.H. Brautigam, K.J. Kerns, P.A. Robinson, and E.G. Holeman, Radiation-Induced Insulator Pulses in the CRRES Internal Discharge Monitor Satellite Experiment, IEEE Trans. Nuc. Sci., 38, 1614 – 1621, 1991.

Frederickson, A.R., E.G. Mullen, K.J. Kerns, P.A. Robinson, and E.G. Holeman, The CRRES IDM Spacecraft Experiment for Insulator Discharge Pulses, IEEE Trans. Nuc. Sci., 40, 233-241, 1993.

Garbe, G.G., and E.E. Montgomery IV, An Overview of NASA's Solar Sail Propulsion Project, 39th AIAA Joint Propulsion Conference, AIAA-2003-5274, 20-23 July 2003.

Garrett, H.B., and S.E. DeForest, An analytical simulation of the geosynchronous plasma environment, Planet. Space Sci., 27, 1101-1109, 1979.

Garrett, H.B., and A. Hoffman, Comparison of Spacecraft Charging Environments at the Earth, Jupiter, and Saturn, in *6th Spacecraft Charging Technology Conference*, AFRL-VS-TR-20001578, 1 September 2000.

Garrett, H.B., D.C. Schwank, and S.E. DeForest, A Statistical Analysis of the Low-Energy Geosynchronous Plasma Environment—1. Electrons, Planet. Space Sci., 29, 1021-1044, 1981.

Hunt-Ward, T., and T.P. Armstrong, Ulysses HISCALE Data Analysis Handbook, Fundamental Technologies, 2003, (http://hiscale.ftecs.com/uly-handbk-oview.html, accessed March 2005).

Johnston, J., B. Ross, J. Blandino, J.Lawrence, and C. Perrygo, Development of Sunshield Structures for Large Space Telescopes, Proceed. SPIE, 4850, 209-220, in *IR Space Telescopes and Instruments*, J.C. Mather, ed., March, 2003.

Kane, M., B.H. Mauk, E.P. Keath, and S.M. Krimigis, Hot ions in Jupiter's magnetodisc: A model for Voyager 2 low-energy charged particle measurements, *J. Geophys. Res.*, 100, 19,473 – 19,486, 1995.

Maksimovic, M., V. Pierrard, and P. Riley, Ulysses electron distributions fitted with Kappa functions, Geophys. Res. Lett., 24, 1151-1154, 1997.

Minow, J.I., W.C.Blackwell,Jr., and A. Diekmann, Plasma Environment and Models for L2, AIAA Paper 2004-1079, 42nd AIAA Aerospace Sciences Meeting and Exhibit, Reno, NV, 5-8 January 2004.

Minow, J.I., W.C. Blackwell, L. Neergaard, S. Evans, D.M. Hardage, and J.K. Owens, "Charged particle environment definition for NGST: L2 plasma environment statistics," in *UV, Optical, and IR Space Telescopes and Instruments*, *Proc. SPIE*, **4013**, J.B. Breckinridge and P. Jakobsen, eds., pp. 942 – 953, 2000.

NASA 1999, Avoiding Problems Caused by Spacecraft On-Orbit Internal Charging Effects, NASA-HDBK-4002, 1999.

NSSDC Users Guide for Data from the Ulysses SWOOPS Plasma Experiment: the positive Ion experiment, (http://helio.estec.esa.nl/ulysses/ftp/data/swoops/ions/readme.txt, accessed Aug 2004).

Rodgers, D.J., DICTAT Software Users' Manual, DERA/CIS/CIS2/SUM991081, Issue 2.0, November 1999.

Rodgers, D.J., K.A. Ryden, G.L. Wrenn, P.M. Latham, J. Sorensen, and L. Levy, An engineering tool for the prediction of internal dielectric charging, in *6th Spacecraft Charging Technology Conference*, AFRL-VS-TR-20001578, September 2000.

Sheldahl, Red Book, Aerospace Thermal Control Materials and Films, Sheldahl Technical Materials, Northfield MN, July 2003, (http://www.sheldahl.com/Product/bulletins/RedBook.pdf, accessed March 2005).

Smart, D.F., and M.A. Shea, Comment on Estimating the Solar Proton Environment that May Effect Mars Missions, Adv. Space Res., 31, 45- 50, 2003.

Swaminathan, P., J.R. Dennison, A. Sim, J. Bruson, E. Crapo, and A.R. Frederickson, Comparison of classical and charge storage methods for determining conductivity of thin film insulators, in *8th Spacecraft Charging Technology Conference*, J. Minor (ed), NASA/CP-2004-2130-91, March 2004.

West, J., and B. Derbès, Solar Sail Vehicle System Design for the Geostorm Warning Mission, AIAA-2000-5326, 2000.

Woolf, N.J., J.R.P. Angel, Passive cooling of gossamer telescopes, Proc. SPIE, 4091, 39-42, in *Imaging Technology and Telescopes*, J.W. Bilbro, J.B. Breckinridge, R.A. Carreras, S.R. Czyzak, M.J., Eckart, R.D. Fiete, and P.S. Idell, eds., October, 2003.